PERGAMON

Quaternary International 65/66 (2000) 3–13

A positive climatic feedback mechanism for Himalayan glaciation

Andrew B.G. Bush

Department of Earth and Atmospheric Sciences, 126 Earth Sciences Building, University of Alberta, Edmonton, Alberta, Canada T6G 2E3

Abstract

Glaciation at elevated sites in low latitudes has the potential to play an important role in the global radiation budget because the magnitudes of incoming and reflected shortwave radiation are so large. A climatic mechanism is presented which provides a positive feedback for glaciation in the Himalayan mountains. A higher bare surface albedo in the Himalayas induces an atmospheric circulation response that consists of cooling and descent over the Himalayas and warming and a contrasting air mass uplift to the west over the Persian Gulf and the Arabian peninsula. Although annual mean rainfall over the subcontinent south of the Himalayas decreases, the summer southwesterly monsoon winds are stronger over the mountains in northwestern India and carry more moisture to higher elevations where it is precipitated as snow. Conversely in wintertime, the northeasterly monsoon winds are weakened over the Himalayas and surface wind convergence and snowfall are increased there. Increased snowfall in the mountains expands the surface area of the high albedo region in both seasons, leading to a positive feedback. The peak amplitude of this feedback is ultimately regulated by springtime melting rates.

1. Introduction

Interactions between the Earth's atmosphere and cryosphere occur on an extraordinarily wide range of time scales and can have dramatic consequences for the global climate. An expansion of continental ice sheets during an ice age, for example, represents an extreme change in the boundary conditions that force the atmosphere (e.g., Broccoli and Manabe, 1987; Manabe and Broccoli, 1985; Hall et al., 1996; Weaver et al., 1998; Bush and Philander, 1999). Both dynamical steering of atmospheric winds by ice sheet topography as well as changes in the radiation budgets at the Earth's surface by highly reflective ice can provide positive feedbacks which promote further ice growth (e.g., Crowley, 1984; Crowley and North, 1991). On a somewhat faster time scale, regions that are seasonally snow-covered experience a snow-albedo feedback which plays an important role in regulating the annual mean climate through modification of the shortwave radiation balance at the surface.

In addition to radiative effects, however, there are dynamical implications to the albedo feedback as strong radiative cooling or warming of the atmosphere provides a forcing mechanism for driving atmospheric winds. At low latitudes, the dynamical response of the atmosphere to anomalous heating or cooling can well be described by linear theory and can be seen primarily as a combination of Rossby and Kelvin waves (Gill, 1980). Off the equator, the Rossby wave response is dominant and is the one on which we will focus in this study. Rossby waves arise from the change in Coriolis parameter with latitude ($f = 2\Omega \sin \Theta$, where Ω is the Earth's rotation rate and Θ is latitude). They propagate to the west (with respect to the mean winds) and in the midlatitudes they are very important because they induce meandering of the upper tropospheric jet. This meandering advects warm subtropical air northward and cold Arctic air southward and helps to equilibrate the differential heating of the Earth's surface.

Anomalous, large-scale heating or cooling in the atmosphere can generate Rossby waves. For example, during the summer monsoon season in southeastern Asia, latent heat release over the Indian subcontinent triggers a Rossby wave response which can impact the climate in distant regions to the west of the source region. In particular, the Rossby wave response is such that a heat source over the Indian subcontinent induces subsidence of the westerly midlatitude jet and drying over Arabia, northeastern Africa and the eastern Mediterranean (Rodwell and Hoskins, 1996). As the response is predominantly linear, a cooling over the Indian subcontinent would induce uplift of the jet to the west. The spatial extent of the response is determined by the strength of the

E-mail address: andrew.bush@ualberta.ca (A.B.G. Bush).

1040-6182/00/$20.00
PII: S1040-6182(99)00033-6

forcing, but for realistic values of latent heating in the monsoon region, Rodwell and Hoskins (1996) have demonstrated that this dynamical atmospheric response is felt more than 60° of longitude to the west.

The low latitude of the Himalayan mountains implies that the subtropical glaciers there receive much more solar radiation than they would at higher latitudes. Measurements have shown that the amount of shortwave radiation intercepted at the surface is approximately four times greater than that intercepted between 60 and 70N (at the elevation of glaciation; Kuhle, 1988). Compared to higher latitudes, any ice-albedo feedback would therefore be greatly amplified and would result in stronger cooling of the atmosphere. This cooling would force an atmospheric circulation anomaly through Rossby waves which could potentially influence the moisture source for the region. The importance of both summertime and wintertime monsoon circulations in regulating the climate in the south Asian region means that any changes to them as a result of anomalous circulations may have a significant impact on the regional climate.

A connection between Eurasian and Himalayan snowfall and monsoon rainfall over the subcontinent has previously been established both by numerical simulations and by direct observations. Modeling studies have demonstrated that summer monsoon rainfall over India is reduced after a winter of excessive snowfall (Hahn and Shukla, 1976). Similarly, observational data suggest that excessive Eurasian snow cover reduces monsoon precipitation (Dickson, 1984). It has also been suggested that Himalayan snow cover may affect the timing of monsoon advance and retreat over the subcontinent, with excessive springtime Himalayan snowfall delaying monsoon advance and excessive summertime snowfall delaying monsoon retreat (Dey and Bhanu Kumar, 1982; Dey et al., 1985). While the latter conclusions have been contested (Ropelewski et al., 1984) it is nevertheless apparent that Himalayan and Eurasian snow cover do have a dynamical impact on the monsoon. In addition, a comparison of late Quaternary glaciations in the Himalayas to paleoclimatic records suggest that there is a link between the summer monsoon, the mid-latitude westerlies and Himalayan glaciation (Benn and Owen, 1998).

In this study we explore a feedback between surface albedo, atmospheric circulation and snowfall in the low latitude region of the Himalayan mountains. We will demonstrate that this feedback is a positive one and that it could play a role in promoting glacial expansion in the region. To investigate the mechanisms behind this feedback, two numerical simulations have been performed using a general circulation model of the atmosphere. The following section describes the atmospheric model and its parameterizations. Section 3 presents the results of the simulations, followed by a discussion in Section 4 and conclusions in Section 5.

2. The model

The atmospheric general circulation model was developed at the Geophysical Fluid Dynamics Laboratory (Princeton, NJ) and is more fully described by Gordon and Stern (1982). The equivalent spatial resolution of the model is 3.75° in longitude and approximately 2° in latitude; there are 14 levels in the vertical (in the figures, level 14 is approximately 30 m above the ground and level 1 is at the top of the model at 50 millibars). Interested readers are referred to the appendix, which gives more technical details on the model and its resolution. Clouds are predicted according to the scheme of Wetherald and Manabe (1988), and seasonal insolation is imposed using modern orbital parameters. Bare land surface albedo is prescribed initially but may be modified by snowfall as it occurs during the simulation. Daily sea surface temperatures are prescribed through an interpolation from monthly mean climatological data (Levitus, 1982) and are the same in both simulations.

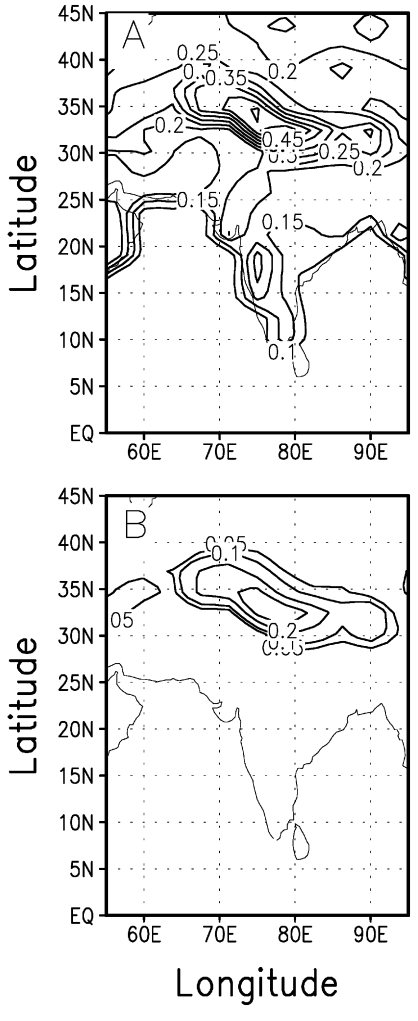

Fig. 1. (A) Bare land surface albedo in the Himalayan region for the present day and (B) the difference in albedo between the two numerical experiments.

In order to determine the impact of low latitude surface albedo on glaciation in the Himalayas the results of two numerical simulations are compared. The only difference between the simulations is in the prescribed bare surface land albedo in the Himalayas. The first simulation has modern surface albedo imposed (Fig. 1A); albedo in the second simulation is different in the region between 56E and 94E longitude, and 26N to 44N latitude, where higher values are prescribed (Fig. 1B shows the difference in albedo). Simulations using these higher albedos are taken to represent the radiative effects of glacial inception but are nevertheless modest when compared to those for actual glacial ice, which are typically 0.6–0.9. The goal of these simulations is to determine whether the feedbacks induced by glacial inception would promote or hinder further glacial expansion. The region chosen is not meant to represent any historical glacial extent. It was chosen so that it would be large enough in areal extent to trigger a large-scale atmospheric response.

3. Results

When modern surface albedo is imposed, simulated surface temperatures over the greater Himalayas (above ~ 4500 m) are typically less than freezing in an annual mean (Fig. 2A). Increasing the surface albedo cools the annual mean temperature over the region by nearly 1° (Fig. 2B) through increased reflected shortwave radiation. To the west of the Himalayas there is an annual mean warming of more than a degree along the coast of the Arabian Sea, over southern Iran and the Arabian

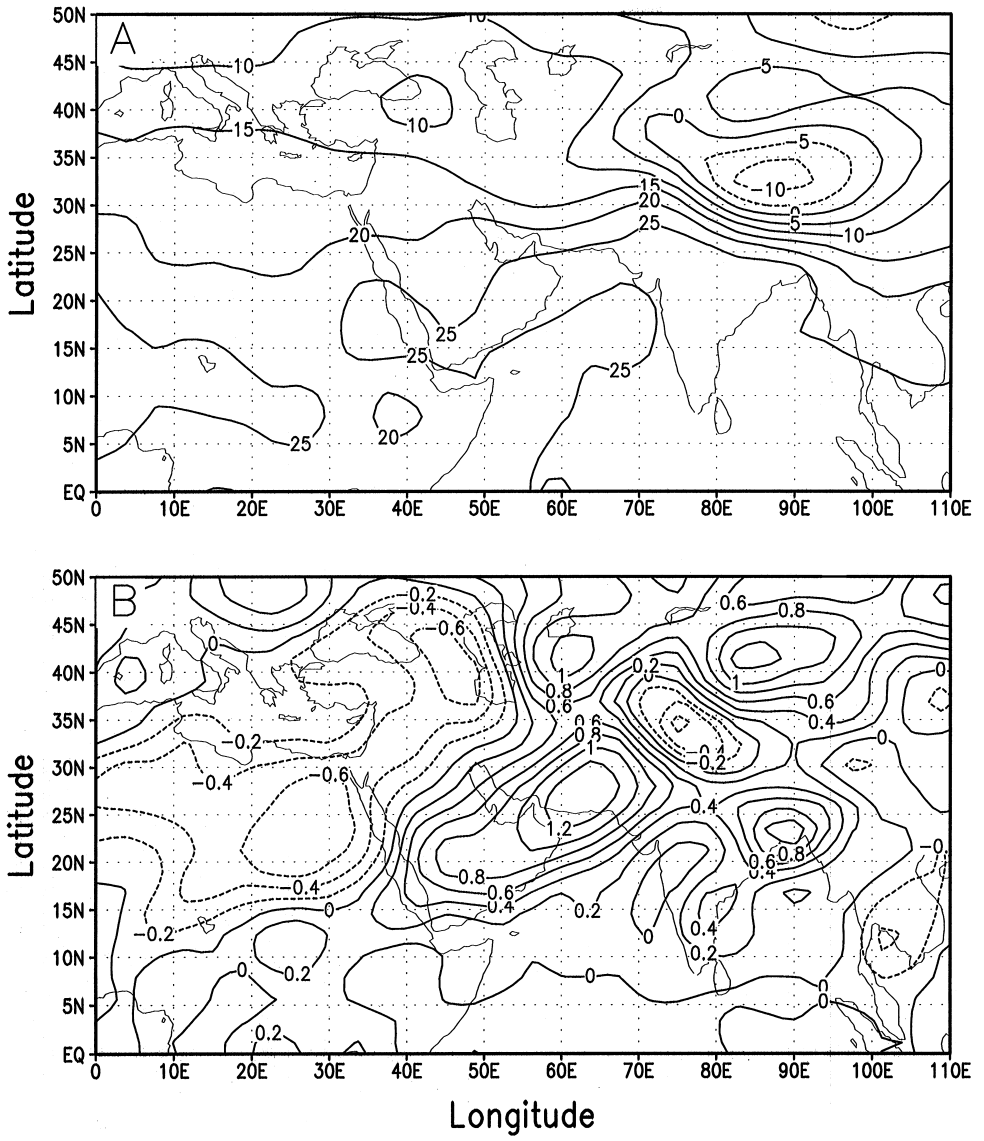

Fig. 2. (A) Annual mean surface temperature in the south Asian monsoon region in the control simulation (degrees Centigrade with a contour interval of 5°). (B) The temperature difference between the two simulations (high albedo experiment minus control). The contour interval is 0.4°.

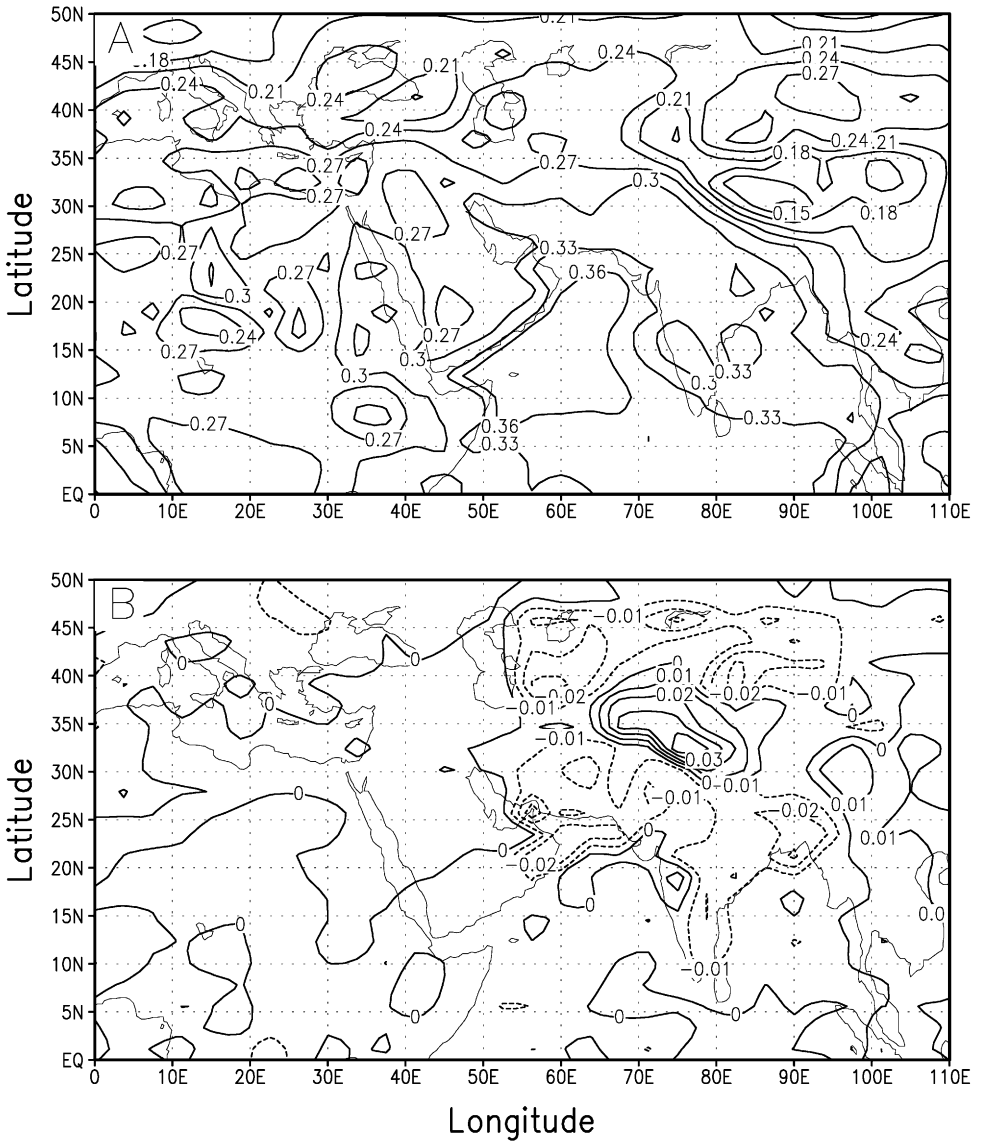

Fig. 3. Annual mean net incoming shortwave radiation at the surface in (A) the control simulation and (B) the difference between the two simulations (control minus high albedo experiment). Units are in cal/cm^2/min with a contour interval of 0.03 cal/cm^2/min in (A) and 0.01 cal/cm^2/min in (B).

peninsula, as well as south of the Aral Sea. Farther to the west over, the northeastern Sahara and the eastern Mediterranean, there is cooling of nearly 1° in the annual mean.

A fraction of these temperature differences may be attributed directly to changes in the radiation balance at the surface. Cooling over the region of increased surface albedo, for example, is primarily through a 50% increase in reflected shortwave radiation (Fig. 3). The warmer area bordering the Himalayas correlates spatially with a net increase in absorbed shortwave radiation, although the net radiative change is typically less than 10% of the modern annual mean value (Fig. 3A). However, the spatial extent of the warming along the Arabian Sea coast and in particular the cooling of the Sahara and the eastern Mediterranean, extends well past the region of direct radiative forcing (cf. Fig. 2). This implies that some of the temperature anomalies in regions remote from the Himalayas are not necessarily directly attributable to radiative forcing. In higher latitudes, the temperature and pressure differences are attributable to changes in the variable midlatitude jet stream; in tropical latitudes, there is little change between the two simulations.

The spatial pattern of cooling/warming/cooling over and to the west of the Himalayas suggests that the atmosphere is responding to the altered surface albedo

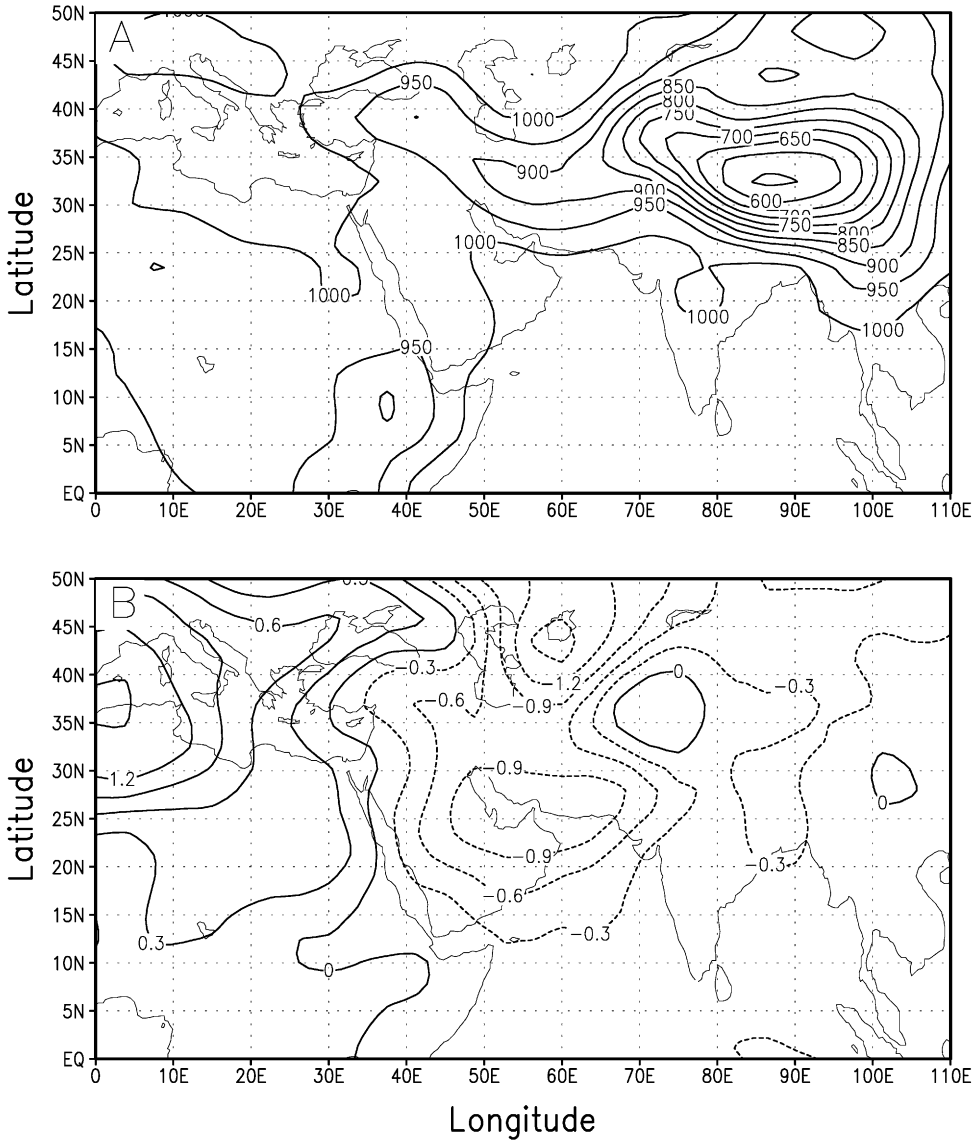

Fig. 4. Annual mean surface pressure in units of millibars in (A) the control simulation and (B) the difference between the two simulations (high albedo experiment minus control). Contour intervals are 50 mb in (A) and 0.3 mb in (B).

through a large-scale wave response and that the patterns of the surface temperature anomalies are a signature of this wave. Differences in the annual mean surface pressure (Fig. 4) correlate spatially with the temperature anomalies: there is higher atmospheric pressure over the region of higher albedo and lower pressure over the warmer Persian Gulf and Aral Sea. The fact that there are pressure anomalies indicates that the atmosphere's response is dynamical in these regions and implies that there are concomitant changes in the strength and direction of the mean winds that bring precipitation to the Himalayas.

The annual mean lower tropospheric winds in the control simulation (Fig. 5A) reveal the dominance of the westerly summer monsoon winds. Differences in the annual mean winds (Fig. 5B) indicate anticyclonic and divergent flow over the Himalayas where the albedo is high, and cyclonic wind anomalies associated with the reduced pressure and warmer temperatures over the Persian Gulf and the Arabian peninsula. Along the northeastern coast of the Arabian Sea, the wind anomalies are in a direction such that the southwesterly summer monsoon winds are strengthened and the northeasterly winter monsoon winds are weakened. The wind differences also indicate much stronger convergence over the northwestern Himalayas in the annual mean.

A seasonal breakdown of the winds indicates that in the summer months of June–July–August the monsoon

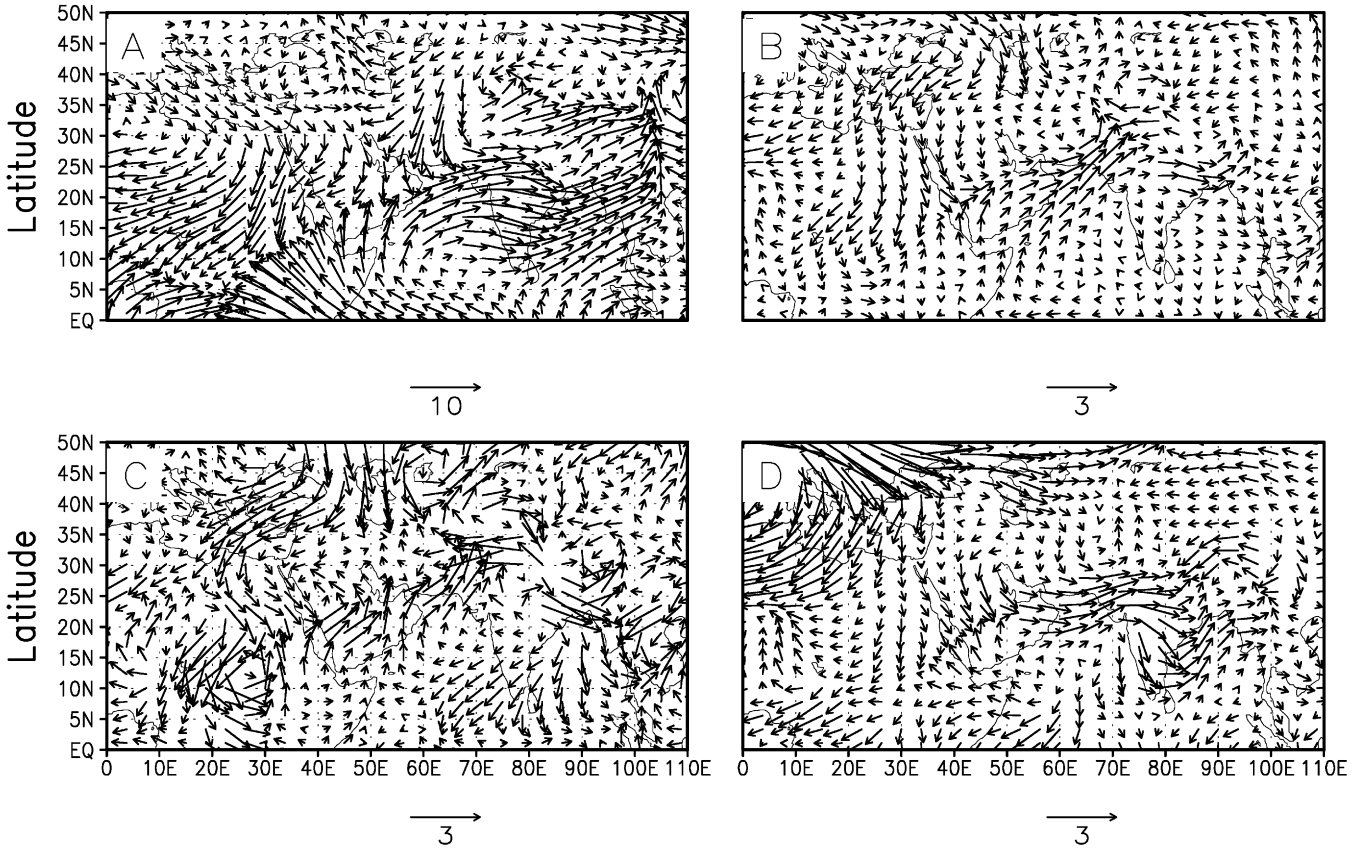

Fig. 5. (A) Annual mean vector winds near the surface in the control simulation. Other panels show the vector wind difference between the two simulations (high albedo experiment minus control) for (B) the annual mean, (C) the June–July–August mean, and (D) the December–January–February mean. The arrows are scaled in m/s as shown below each frame.

winds, strengthened by the anomalous cyclonic circulation along the Arabian Sea coast, increase low-level convergence over the northwestern Himalayas near 70E, 30N (Fig. 5C). Conversely, in the winter months of December–January–February the northeasterly monsoon winds, weakened by the anomalous circulation along the Arabian Sea coast, increase convergence over the eastern Himalayas (Fig. 5D). The magnitude of the wind speed changes is on the order of 1–3 m/s, which represents an approximate 10% change in the strength of the monsoon winds.

A consequence of increased low level wind convergence over the Himalayas in both summer and winter is that the net snowfall increases by more than 2 cm (water equivalent) in places, an approximate 50% increase (Fig. 6). Enhanced snowfall in the northwestern Himalayas is caused primarily by the increased convergence of the summer monsoon winds (cf. Fig. 5C), whereas the increase in the southeastern Himalayas is caused by convergence of the winter monsoon winds.

More snowfall accumulation in the Himalayas also increases the areal extent of higher albedo values (Fig. 7). In addition, fresh snow increases even further the annual mean surface albedo in the region whose bare surface albedo was initially prescribed to be greater (compare Figs. 1 and 7).

There is thus a positive feedback; higher surface albedo induces an atmospheric response whose pressure anomalies change the monsoon winds in such a way that low level convergence over the region is increased, snowfall increases and the surface area of the high albedo region increases. The dynamics of the atmospheric response will be examined in the next section along with the processes which ultimately regulate the amplitude of this feedback.

4. Discussion

The relationship between enhanced Himalayan glaciation and monsoon wind strength does not appear to be quite so straightforward as the view that anticyclonic winds around the glaciated region decrease the strength of the summer monsoon winds. While anticyclonic winds do occur over the region in the simulation, they do not extend sufficiently far south to affect the monsoon winds directly (cf. Fig. 5B).

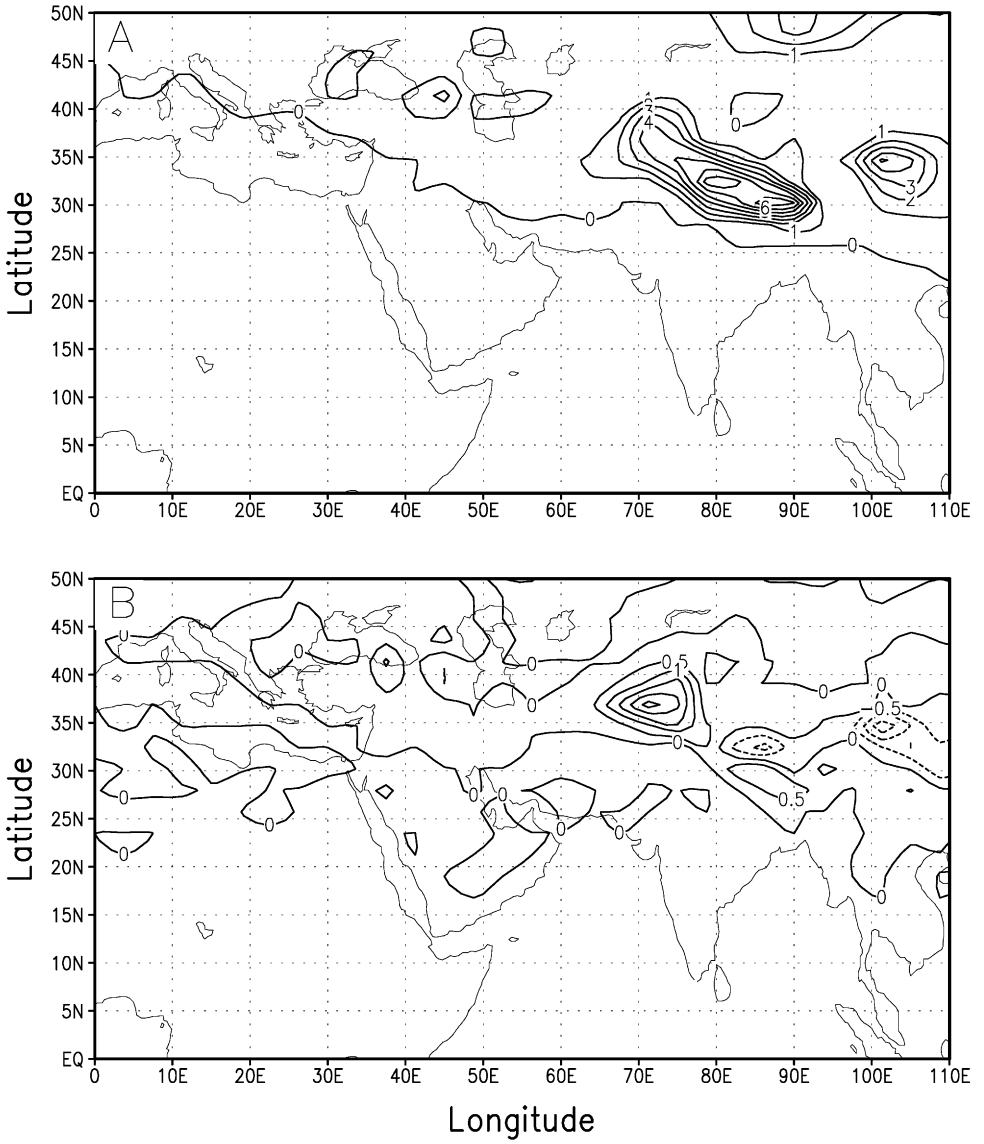

Fig. 6. (A) Annual mean snowfall in the present day simulation and (B) the difference between the two simulations (high albedo experiment minus control). Units are in centimeters water equivalent with contour intervals of 1 cm in (A) and 0.5 cm in (B).

There is, however, an atmospheric response to the surface albedo change which is nonlocal and which does influence the monsoon winds. This atmospheric response is in the form of a large-scale, subtropical Rossby wave whose surface signature is reflected in the temperature, pressure and wind fields to the west of the source region and whose vertical circulation pattern reveals the wave's structure (Fig. 8A). The wavelength is approximately 10° of longitude, and the structure of the wave persists over 40–50° of longitude to the west of the Himalayas. However, both the wavelength and the amplitude of the wave change throughout the year since the strength of the forcing is dependent on the seasonal insolation. In an annual mean of temperature, the wave's surface signature is seen most clearly in the warming and uplift to the west of the Himalayas over the Persian Gulf and the Arabian peninsula (Fig. 8B).

The generation mechanism for these Rossby waves is as follows. In the simulation, increased surface albedo in the Himalayas induces anticyclonic and divergent surface winds. Above this surface divergence there is strong descent and a compensating convergence in the upper troposphere (Fig. 9). Anomalously strong wind convergence in the upper troposphere acts as a source for triggering Rossby waves (Sardeshmukh and Hoskins, 1988; Grotjahn, 1993). Through a calculation of the magnitude of each of the possible forcing terms (Grotjahn, 1993), it is seen in the present study that this enhanced upper level wind convergence is the dominant mechanism by which these waves are generated.

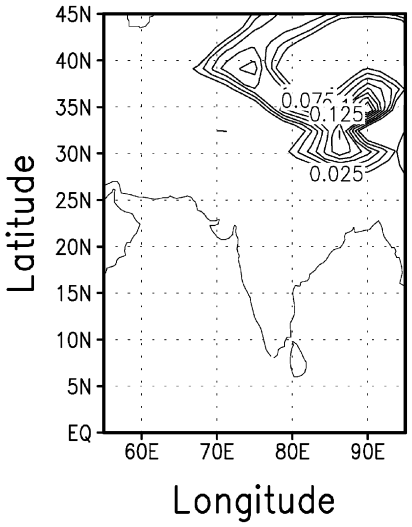

Fig. 7. Change in surface albedo during the experiment. The contour interval is 0.025.

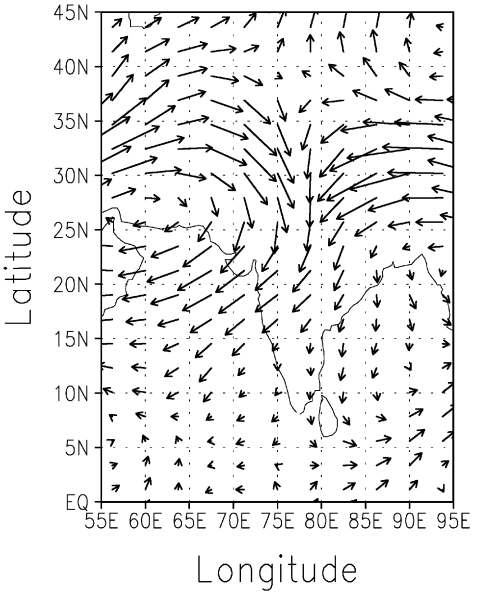

Fig. 9. Annual mean vector wind difference in the upper troposphere over the Himalayas (high albedo experiment minus control).

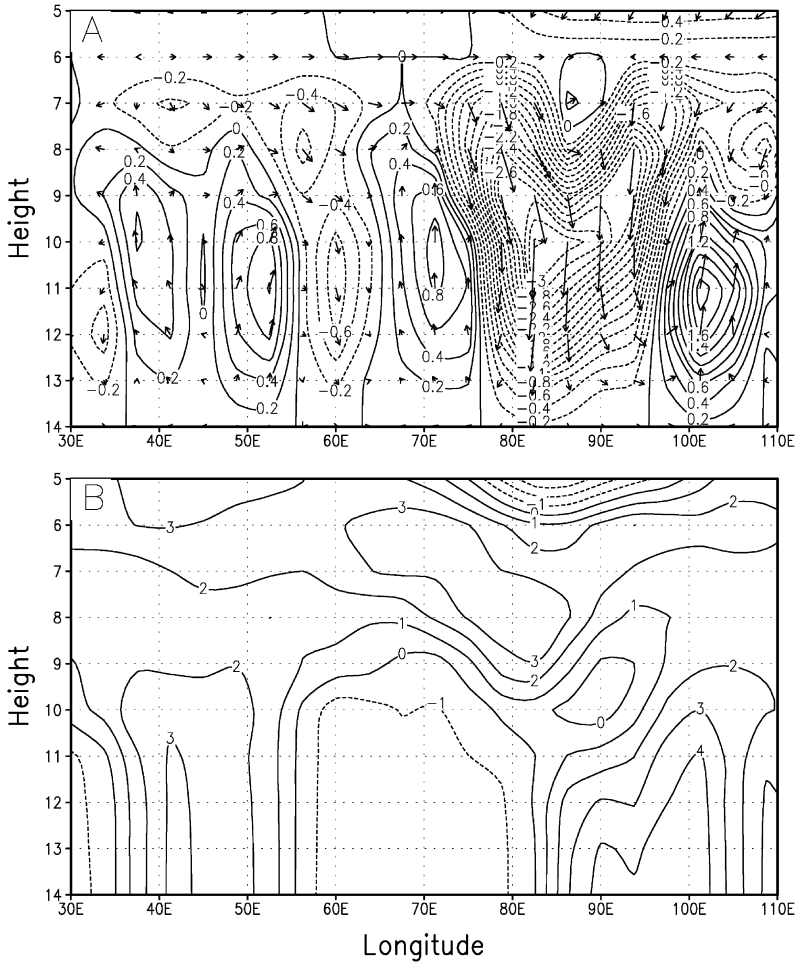

Fig. 8. (A) A height-longitude cross-section of the May atmospheric circulation anomaly at latitude 30N (arrows) with the difference in vertical velocity of pressure surfaces shown in contours (units are 10^{-7} s^{-1}). (B) The temperature difference in the same vertical plane, with a contour interval of 1°. (The vertical levels in the model are such that level 14 is approximately 30 meters above the ground and level 1 is at 50 millibars; the top of the troposphere is approximately at level 5.)

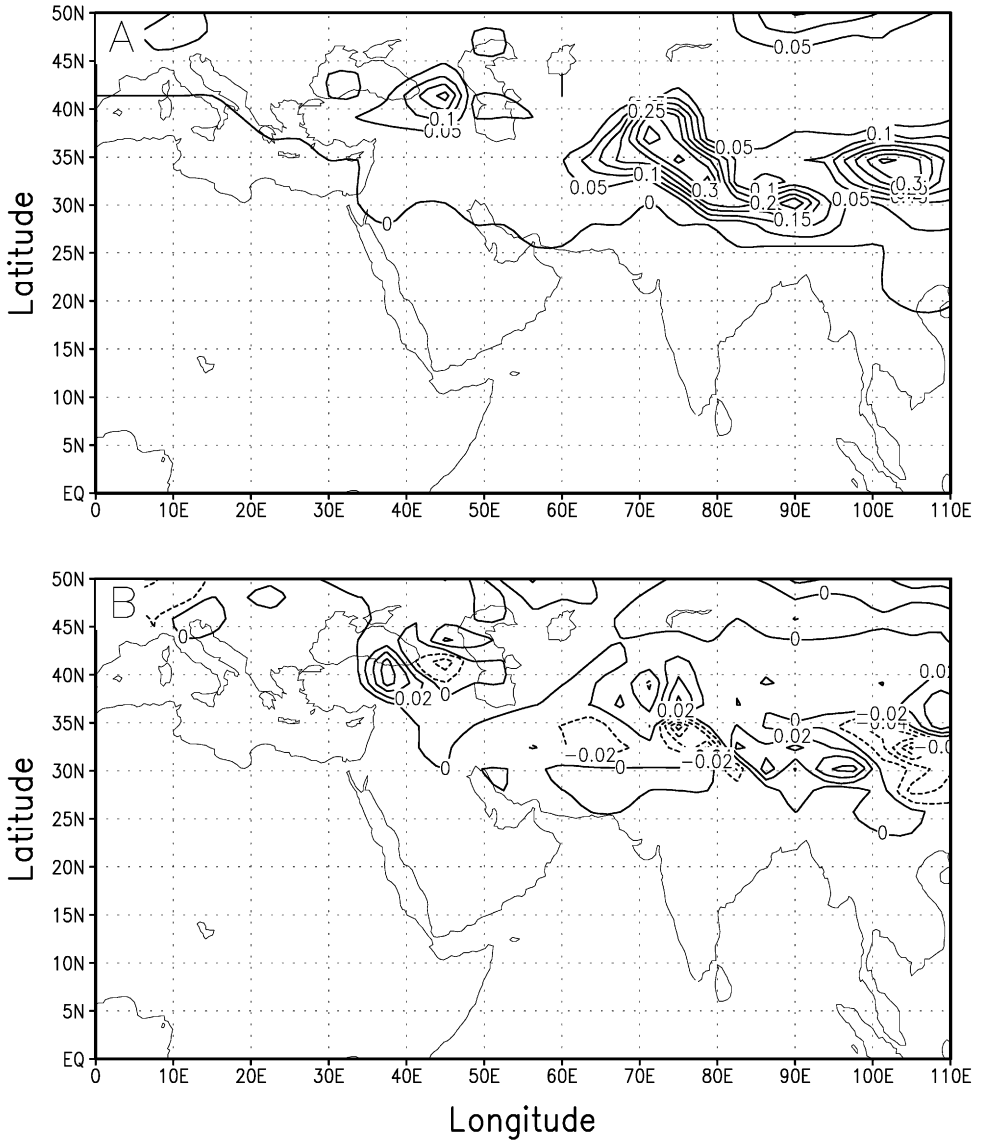

Fig. 10. (A) March–April–May snowmelt rates (cm/day equivalent) for the present day simulation (contour interval 0.05 cm/day) and (B) the difference between the two simulations (contour interval 0.02 cm/day).

The effect of these waves to the west of the forcing region spans approximately 20° of subtropical latitude with increased temperatures extending from the Arabian Sea to the Aral Sea. In higher latitudes, temperature differences between the simulations are associated with the meandering midlatitude westerly jet. Warming of the Persian Gulf and of the eastern Arabian peninsula impacts both the summer and the winter monsoon winds, as described in the previous section, by increasing surface convergence over the Himalayas in both seasons. This feedback is potentially important for glacial inception in the Himalayas because if, for example, the albedo is increased through an initial buildup of ice — perhaps through decadal or centennial climate variability — then the dynamical response of the atmosphere is such that the albedo is further increased and the glaciated area is expanded by enhanced snowfall.

This feedback is ultimately limited in the model by the snowmelt rates. In particular, springtime snowmelt increases in the simulation so that the excess winter snow accumulation melts primarily in the March–April–May season (Fig. 10), with melting rates more than 10% greater in places.

The fact that snowfall increases over this particular region of the Himalayas does not contradict the observational conclusions linking greater snow cover to reduced mean monsoon precipitation. In the simulation, precipitation over the Indian subcontinent in the area between 70E–90E longitude and 5N–30N latitude decreases by approximately 6%, a change that is consistent with

observational conclusions (Dickson, 1984). Nevertheless, for the purposes of glacial inception it is the spatial variability of the precipitation changes — in particular the changes over a localized region of the Himalayas — that is important and not necessarily the spatial mean over the Indian subcontinent. These simulations demonstrate that the local and nonlocal feedbacks between the atmosphere and the underlying land surface in the Himalayas can act in a way that may not at first be obvious from conclusions drawn from spatially averaged data.

Some other factors which can also influence monsoon strength but which have not been taken into account in these simulations will now be discussed. The state of the tropical Pacific Ocean affects monsoon strength since there is a strong correlation of weak monsoons with El Niño and strong monsoons with La Niña (e.g., Keshavamurty, 1982; Bush, 1999). On longer time scales, it is well known that changes in the Earth's orbital parameters have a dramatic impact on the strength of the monsoon such that increased seasonality drives stronger monsoon winds (e.g., Prell and Kutzbach, 1992). Glacial periods also affect monsoon strength; in a simulation with a coupled atmosphere–ocean model, the strength of the monsoon westerlies is increased but colder global temperatures and colder Indian Ocean temperatures reduce their moisture content (Bush and Philander, 1999). There are thus many factors which can influence the monsoon. In numerical simulations, the glacial monsoon shows the largest wind changes whereas those induced by tropical Pacific sea surface temperature anomalies and those induced by orbital changes are comparable to those seen in this study. In reality, monsoon strength will be determined by a combination of all of these factors.

5. Conclusions

The results of two numerical simulations suggest that a positive feedback can occur in the atmosphere–cryosphere system which may be important in promoting glacial expansion in the Himalayas. Increasing the surface albedo induces strong descent with concomitant upper level convergence. This upper level convergence forces a seasonally-dependent atmospheric Rossby wave response which alters the low level temperature and pressure fields to the west of the mountains in such a way as to modify the monsoon winds and increase low-level wind convergence and snowfall in the mountains in both summertime and wintertime. The surface area of increased albedo thereby expands, leading to a positive feedback. This process is regulated by springtime melting rates, which are sufficiently high that most of the excess snow cover is melted away before the following winter.

The model simulations do not capture longer time scale (decadal, centennial) climate variability which could potentially be responsible for initiating the feedback process. Nevertheless, the feedbacks that do occur in the model indicate that the connection between Himalayan snow cover and the atmospheric response is a subtle one with both local and nonlocal effects playing important roles. These processes may have been important to the advance or retreat of Quaternary glaciations in the region.

Acknowledgements

The author thanks Jim Teller and Dougie Benn for very helpful comments in their reviews. The author gratefully acknowledges the support of a National Sciences and Engineering Research Council of Canada grant OGP0194151 and NSERCs Climate System History and Dynamics Research Network grant. This work was performed for the UNESCO sponsored International Geological Correlation Project number 415.

Appendix A

The atmospheric general circulation model is spectral in the horizontal. Spectral models describe atmospheric variables (such as temperature, velocity, etc.) not by values at discrete points but rather by a summation of a series of waves (analogous to a Fourier series). The summation is over a number of waves of differing wavelengths ranging from planetary scale down to hundreds of kilometers. In these simulations, rhomboidal truncation is applied with the maximum number of zonal waves being 30. This gives an equivalent spatial resolution of 3.75° in longitude and approximately 2° in latitude (although for rhomboidal truncation the equivalent meridional resolution changes with latitude such that there is higher resolution near the poles). Topography in the model must be smoothed in order to be compatible with the spectral resolution.

In the vertical plane the model is finite-differenced with 14 unevenly spaced σ-levels at $\sigma = 0.015, 0.05, 0.101, 0.171, 0.257, 0.355, 0.46, 0.568, 0.676, 0.777, 0.866, 0.935, 0.979$, and 0.997 (where σ is a normalized pressure coordinate defined by $\sigma = P/P^*$, where P^* is the surface pressure). This normalized pressure coordinate is used so that surface topography does not intersect the model levels; this would not be the case if actual pressure coordinate were used. In a standard atmosphere, the sigma = 0.997 surface would always be ~ 30 m above the ground.

In order to perform spatially localized physical calculations such as radiation, cloud formation, precipitation, evaporation, etc., the model converts the spectral variables to grid variables (i.e., the variables are now defined

on a latitude-longitude grid) using a fast Fourier transform. Once these calculations are performed the model then converts the grid variables back to spectral variables and advances them forward in time according to the hydro- and thermodynamical prediction equations using a time step of 216 s. For lower-resolution models, spectral methods have realized large savings in computational efficiency.

Sea surface temperatures in this model are prescribed as described in Section 2. Thus, the ocean does not respond to any changes in atmospheric circulation and coupled atmosphere–ocean phenomena such as El Niño are thereby precluded.

References

Benn, D.I., Owen, L.A., 1998. The role of the Indian summer monsoon and the mid-latitude westerlies in Himalayan glaciation: review and speculative discussion. Journal of Geological Society 155, 353–363.

Broccoli, A.J., Manabe, S., 1987. The influence of continental ice, atmospheric CO_2, and land albedo on the climate of the last glacial maximum. Climate Dynamics 1, 87–99.

Bush, A.B.G., 2000. Orbital forcing versus sea surface temperature forcing and the implications for early Holocene climate. Quaternary Research, submitted for publication.

Bush, A.B.G., Philander, S.G.H., 1999. The climate of the Last Glacial Maximum: results from a coupled atmosphere-ocean general circulation model. Journal of Geophysical Research, 104, 24509–24525.

Crowley, T.J., 1984. Atmospheric circulation patterns during glacial inception: A possible candidate. Quaternary Research 21, 105–110.

Crowley, T.J., North, G.R., 1991. Paleoclimatology. Oxford Monographs on Geology and Geophysics, Vol. 18, Oxford University Press, New York, 339 pp.

Dey, B., Bhanu Kumar, O.S.R.U., 1982. An apparent relationship between Eurasian spring snow cover and the advance period of the Indian summer monsoon. Journal of Applied Meteorology 21, 1929–1932.

Dey, B., Kathuria, S.N., Bhanu Kumar, O.S.R.U., 1985. Himalayan summer snow cover and withdrawal of the Indian summer monsoon. Journal of Climatology and Applied Meteorology 24, 865–868.

Dickson, R.R., 1984. Eurasian snow cover versus Indian monsoon rainfall — an extension of the Hahn-Shukla results. Journal of Climatology and Applied Meteorology 23, 171–173.

Gill, A.E., 1980. Some simple solutions for heat-induced tropical circulation. Quaternary Journal of Royal Meteorological Society 106, 447–462.

Gordon, C.T., Stern, W., 1982. A description of the GFDL global spectral model. Monthly Weather Review 110, 625–644.

Grotjahn, R., 1993. Global Atmospheric Circulations. Observations and Theories. Oxford University Press, New York, 430 pp.

Hahn, D.G., Shukla, J., 1976. An apparent relationship between Eurasian snow cover and Indian monsoon rainfall. Journal of Atmospheric Science 33, 2461–2462.

Hall, N.M.J., Valdes, P.J., Dong, B., 1996. The maintenance of the last great ice sheets: a UGAMP GCM study. Journal of Climatology 9, 1004–1019.

Keshavamurty, R.N., 1982. Response of the atmosphere to sea surface temperature anomalies over the equatorial Pacific and the teleconnections of the Southern Oscillation. Journal of Atmospheric Science 39, 1241–1259.

Kuhle, M., 1988. The Pleistocene glaciation of Tibet and the onset of ice ages — an autocycle hypothesis. Geological Journal 17 (4), 581–595.

Levitus, S., 1982. Climatological atlas of the world ocean, NOAA Prof. Paper 13, 173 pp., US Government Printing Office, Washington, DC.

Manabe, S., Broccoli, A.J., 1985. The influence of continental ice sheets on the climate of an Ice Age. Journal of Geophysical Research 90, 2167–2190.

Prell, W.L., Kutzbach, J.E., 1992. Sensitivity of the Indian monsoon to forcing parameters and implications for its evolution. Nature 360, 647–652.

Rodwell, M.J., Hoskins, B.J., 1996. Monsoons and the dynamics of deserts. Quaternary Journal of Royal Meteorological Society 122, 1385–1404.

Ropelewski, C.F., Robock, A., Matson, M., 1984. Comments on an apparent relationship between Eurasian spring snow cover and the advance period of the Indian summer monsoon. Journal of Climatology and Applied Meteorology 23, 341–342.

Sardeshmukh, P., Hoskins, B.J., 1988. The generation of global rotational flow by steady idealized tropical divergence. Journal of Atmospheric Science 45, 1228–1251.

Weaver, A.J., Eby, M., Fanning, A.F., Wiebe, E.C., 1998. Simulated influence of carbon dioxide, orbital forcing and ice sheets on the climate of the Last Glacial Maximum. Nature 394, 847–853.

Wetherald, R.W., Manabe, S., 1988. Could feedback processes in a general circulation model. Journal of Atmospheric Science 45, 1397–1415.